

# Long-term measurements of surface fluxes above a Scots pine forest in Hyytiälä, southern Finland, 1996–2001

Tanja Suni<sup>1)</sup>, Janne Rinne<sup>1)</sup>, Anni Reissell<sup>1)</sup>, Nuria Altimir<sup>2)</sup>,  
Petri Keronen<sup>1)</sup>, Üllar Rannik<sup>1)</sup>, Miikka Dal Maso<sup>1)</sup>, Markku Kulmala<sup>1)</sup>  
and Timo Vesala<sup>1)</sup>

<sup>1)</sup> *Department of Physical Sciences, P.O. Box 64, FIN-00014 University of Helsinki, Finland*

<sup>2)</sup> *Department of Forest Ecology, P.O. Box 27, FIN-00014 University of Helsinki, Finland*

Suni, T., Rinne, J., Reissell, A., Altimir, N., Keronen, P., Rannik, Ü., Dal Maso, M., Kulmala, M. & Vesala, T. 2003: Long-term measurements of surface fluxes above a Scots pine forest in Hyytiälä, southern Finland, 1996–2001. *Boreal Env. Res.* 8: 287–301. ISSN 1239-6095

We present nearly six years of measurements of surface fluxes of momentum, sensible heat, water vapour, carbon dioxide and aerosol particles, along with a three-month time series of ozone flux, measured by eddy covariance above a Scots pine forest in southern Finland from April 1996 to December 2001. The results show marked seasonal and diurnal variation and a significant effect of local and remote anthropogenic pollution on CO<sub>2</sub> and particle data. The flux of inert CO<sub>2</sub> followed environmental factors through plant and soil-microbe metabolism very closely. The flux of reactive O<sub>3</sub> depended on the overlapping influences of environmental parameters driving photosynthesis and of the available amount of reaction partners. The flux of multireactive aerosol particles showed no clear connection with any environmental variable. On new-particle-formation days, the average deposition velocity of particles was, however, greater than usual because small nucleation-mode particles have greater deposition velocities than do larger accumulation-mode particles.

## Introduction

The biosphere and the atmosphere form a coupled, complex, non-linear system, the components of which interact by exchanging momentum, heat, gases and particles. The vertical flux of momentum ( $F_m$ ) is a measure of the friction

that the surface inflicts on air masses moving above it. This friction effect is confined to the atmospheric boundary layer (ABL), the dynamics of which affect all surface fluxes. In the deep daytime boundary layer, concentrations of gases and particles are mixed effectively. At night, the boundary layer is shallow with mixing less effec-

tive. Consequently, the net emission or deposition of gases and particles exerts a larger influence on concentrations within and just above the forest at night than in daytime, potentially resulting in night-time accumulation or depletion of different species. Concentration profiles may then change abruptly in the morning when the mixing begins again. This dilution of accumulated species or the replenishment of depleted species in the morning is especially important in boreal coniferous forests where the ABL often grows markedly higher than, for instance, in temperate forests (Baldochi and Vogel 1996).

Sensible heat and water vapour (latent heat) fluxes ( $F_H$ ,  $F_w(F_{LE})$ ) are major contributors to the ecosystem energy balance, the key to the nature and development of the ABL (Shaw and Finnigan 2002).  $F_w$  above a forest is equivalent to the *evapo-transpiration* of the site, that is, the sum of *transpiration* by vegetation and *evaporation* from the surfaces. Both of these depend on temperature, radiation, soil moisture and vapour pressure deficit (VPD), but, unlike evaporation, transpiration is biologically controlled. The relative contributions of evaporation and transpiration to  $F_w$  vary: On dry summer and autumn days, the diurnal cycle of  $F_w$  above a boreal forest is attributable mostly to plant transpiration (Sevanto *et al.* 2001), whereas after precipitation events and in winter and spring, evaporation from wet ground or snow becomes significant.

Excluding the effect of local anthropogenic pollution, the flux of  $CO_2$  ( $F_C$ ) above a forest is equal to the net ecosystem exchange of  $CO_2$  (NEE), a sum of both plant gross primary production (GPP) driven by photosynthesis, and total ecosystem respiration (TER). Carbon dioxide ( $CO_2$ ) is an *inert* gas that does not take part in chemical reactions in the atmosphere. The diurnal behaviour of NEE is therefore mainly controlled by plant and soil metabolic activity. In the boreal zone, photosynthesis occurs in sunlight during the growing season and, to a very small extent, also during warm spells in evergreen forests in wintertime. Usually, however, it is inhibited in boreal winters (Ottander *et al.* 1995). Release of  $CO_2$  results from respiration that takes place in all living plant cells, including the leaves, branches, stems, roots and mycorrhizae; respiration by microorganisms within the

soil is also important. The relative contribution of these constituents changes in the course of the year according to soil and air temperature, plant tissue age and physiological condition, moisture conditions and the amount of respirable starch or sugar (Kramer and Kozlowski 1979, Högberg *et al.* 2001). At boreal latitudes, overall soil respiration typically diminishes but continues in wintertime, because the thick snow cover insulates the soil and prevents freezing soil temperatures.

Tropospheric concentrations of ozone ( $O_3$ ), a greenhouse gas that is potentially toxic to living organisms, are globally increasing (Volz and Kley 1988). Stomatal uptake is an important sink of  $O_3$ , and the toxicity of  $O_3$  to plants depends not only on episodes of high  $O_3$  concentrations leading to large  $O_3$  fluxes ( $F_{O_3}$ ) but also on accumulated doses. Although boreal forests do not experience the highest ambient concentrations, they rarely experience water stress and are therefore able to sustain high stomatal conductances that can lead to high cumulative doses (Simpson *et al.* 2002). Tropospheric  $O_3$  concentrations depend mainly on a regional photochemical production in the presence of volatile organic compounds (VOCs), nitric oxides ( $NO_x = NO + NO_2$ ), and sunlight, on the intrusion of  $O_3$ -rich air from the stratosphere, and on deposition onto the surface of vegetation and ground (e.g. Jenkin and Clemitshaw 2000).  $O_3$  is *reactive*: It is destroyed upon contact with surfaces as well as in gas-phase reactions. Some of the products of these reactions have very low vapour pressures, and through them  $O_3$  indirectly takes part in the formation of aerosols.

Aerosol particles affect the climate directly by reflecting or absorbing solar radiation and indirectly by acting as cloud condensation nuclei. Either way, aerosols reduce the amount of solar radiation reaching the surface and, consequently, influence  $F_H$  and  $F_w$  and the evolution of the ABL (Yu *et al.* 2002). There is also some indication that the deposition of hygroscopic salt particles on leaf surfaces may have an effect on stomatal water transport processes (Burkhardt *et al.* 2001). A typical, highly hygroscopic ambient aerosol is NaCl (Hämeri *et al.* 2001).

In addition to chemical reactions, physical, meteorological and biological factors enter into the life cycles of *multireactive* aerosol particles.

Their formation and growth are related to the properties and transport of air masses, as well as to biological activity, depending in a highly non-linear fashion on the concentrations of the nucleating and condensing vapours, temperature and relative humidity (Raes *et al.* 2000, Kulmala *et al.* 2000a, Kulmala *et al.* 2000b, Kulmala *et al.* 2001, Mäkelä *et al.* 2002, O'Dowd *et al.* 2002). Terpenes that are emitted by the vegetation are likely to lead to aerosol formation. Their own volatility is too high for direct condensation on the surface of existing aerosol particles, but through reactions with atmospheric oxidants  $O_3$ , OH, and  $NO_3$  (Atkinson 2000), they form products with low volatility and high molecular weight that readily take part in gas-to-particle conversion (Calogirou *et al.* 1999, Atkinson 2000, Raes *et al.* 2000, Jenkin and Clemitshaw 2000). Pinic acid, for instance, a degradation product of both  $\alpha$ - and  $\beta$ -pinene, is probably very involatile and is likely to contribute to secondary aerosol by nucleation or condensation (Raes *et al.* 2000, Jenkin and Clemitshaw 2000, Janson *et al.* 2001).  $\alpha$ -pinene is a major constituent in monoterpene fluxes in Hyytiälä (Rinne *et al.* 2000, Janson *et al.* 2001).

Field measurements of particle, trace gas and other surface fluxes are rarely made continuously and simultaneously over several years. However, the annual variation of most surface fluxes in boreal field conditions is extreme, and little information on the annual behaviour and budgets can be gained from short-term measurements. Long-term field measurements encompassing periods of extreme conditions such as drought or very cold winters are essential also for purposes of global change modelling (Grelle *et al.* 1999). The aim of this paper is to present field measurements of surface fluxes ( $F_m$ ,  $F_H$ ,  $F_w$ ,  $F_C$ ,  $F_{O_3}$ ,  $F_p$ ) made by the eddy covariance technique above a Scots pine forest in southern Finland in 1996–2001. The measurements were continuous over the six years except for  $F_p$  and  $F_{O_3}$ : The time series of  $F_p$  was sporadic and the measurements of  $F_{O_3}$  began in August 2001. Previously, Markkanen *et al.* (2001) have reported  $F_C$ ,  $F_H$  and  $F_{LE}$  for 1996–1999. Similarly, Buzorius *et al.* (1998 and 2000) reported short-term aerosol particle data for summer 1996 and spring 1997. In this paper, we first analyse the annual and diurnal

patterns of the fluxes, present the annual cumulative NEE calculated by two different methods, and investigate the significance of local and remote anthropogenic pollution. Secondly, we focus on the comparison of fluxes and deposition velocities of  $CO_2$ ,  $O_3$ , and aerosol particles. These are atmospheric constituents with very different characteristics, the first being an inert and the second a reactive trace gas, and the multi-reactive particles taking part in chemical, physical and biological processes. Finally, we show the connection between new-particle formation events and particle deposition velocity ( $v_{dp}$ ).

## Material and methods

### Site description

The SMEAR II station is located in a homogeneous Scots pine stand (*Pinus sylvestris* L.), planted in 1962 next to the Hyytiälä forest station in southern Finland (61°51'N, 24°17'E, 181 m above sea level). As 29% of the forests in southern Finland, the Scots pine forest in Hyytiälä is of medium site quality (Vaccinium type according to the Cajander site class system (Cajander 1909) and has a typical growth rate of 8 m<sup>3</sup> ha<sup>-1</sup> yr<sup>-1</sup>. The forest is half way through the rotation time for this site type, which is about 80 years. In 56% of the forest area in southern Finland, the dominating species is Scots pine. Regeneration and growth of the forest have been performed along standard silvicultural guidelines (Peltola 2001).

The height of the dominant stand is around 14 m and the all-sided needle area 8 m<sup>2</sup> m<sup>-2</sup> (2002). The tree biomass is 68 t ha<sup>-1</sup> (above- and below-ground) (Ilvesniemi and Liu 2001). The homogeneous fetch in the prevailing wind direction (230°) is 250 m (Vesala *et al.* 1998). The soil is composed of sandy and coarse silty glacial till. The annual mean temperature in 1961–1990 was +2.9 °C and the annual mean precipitation 709 mm.

### Measurements

At the SMEAR II station, the eddy covariance (EC) measurements of  $F_m$ ,  $F_H$ ,  $F_w$ ,  $F_C$ , and  $F_p$  are

carried out in a tower at the height of 23.3 m and partly at the height of 46.0 m.  $F_{O_3}$  measurements have been carried out at the height of 22.0 m in a second measurement tower since August 2001.

We calculated the EC fluxes as 30-minute averages of the covariance of vertical wind speed and the considered scalar, such as a gas concentration. The measurement system in the tower consists of an ultrasonic 3-D fast-response anemometer (Solent 1012R2, Gill Ltd., Lymington, Hampshire, England) and a fast-response infrared absorption gas analyser (LI-6262 CO<sub>2</sub>/H<sub>2</sub>O analyser, Li-Cor Inc., Lincoln, NE, USA). We estimated the CO<sub>2</sub> storage term (the accumulation of CO<sub>2</sub>) by means of gas gradient measurements at the heights of 4.2, 8.4, 16.8, 23.3, 33.6, and 46.0 m with an infrared absorption analyser (URAS 4, Hartmann & Braun, Frankfurt am Main, Germany). Air temperature fluctuations are calculated from the speed of sound measured with the anemometer. The particle EC system consists of the above-mentioned anemometer at the height of 23.3 m and a condensational particle counter (CPC) TSI model 3010 (lower detection limit ~14 nm). A 4.5-m-long stainless steel tube (inner diameter 3.6 mm) feeds the air from near the anemometer into the CPC, which is located in a box attached to the tower. Vesala *et al.* (1998) describe the measuring system and the site in more detail, and the post-processing procedure of  $F_p$  is presented in Buzorius *et al.* (1998) and that of  $F_c$  and  $F_w$  in Rannik (1998).

The measurement system for  $F_{O_3}$  in the second tower consists of a fast-response acoustic anemometer (Solent HS1199 Research ultrasonic anemometer, Gill Ltd., Lymington, Hampshire, England) and a fast response chemi-luminescence O<sub>3</sub> analyser (LOZ-3 Ozone analyser, Unisearch Associates Inc., Concord, Ontario, Canada). The set-up is, in principal, the same as is described for the CO<sub>2</sub> and H<sub>2</sub>O system in Vesala *et al.* (1998) and so we describe only the main differences here. The anemometer is installed at the height of 22.0 m by means of the 18-m-tall tower and a 6-m-long rectangular installation mast. The box sheltering the gas analyser is installed at a height of 15 m. The (main) sample line is a 10-m-long Teflon® PTFE tube (inner diameter 8 mm). The flow rate in this line is 233 cm<sup>3</sup> s<sup>-1</sup> (T = 273 K, p = 1013 hPa) and it

is controlled by a critical orifice. The analyser is connected to the main line with a 0.5-m-long Teflon® FEP tube (inner diameter 1.58 mm). The flow rate in this line is 16.7 cm<sup>3</sup> s<sup>-1</sup> (T = 273 K, p = 1013 hPa), and it is controlled by a capillary inside the O<sub>3</sub> analyser. Keronen *et al.* (2003) has presented the O<sub>3</sub> measurements in more detail.

The aerosol size distribution measurements in Hyytiälä are performed with a differential mobility particle sizer (DMPS), which has a detection range of 3–600 nanometers in particle diameter. On approximately 50 days per year, the size distributions show a clear increase in the concentration of ultrafine particles (3–20 nm). Subsequently, the newly formed particles often grow to larger sizes by condensation.

From the DMPS size distribution plots, we divided the particle formation events visually into three different classes according to their strength and clarity. Class 1 events include days with an appearance and growth of a distinct nucleation mode which persists for several hours. We classify events with few new particles, a large background concentration, or non-continuous growth as class 2 events. If new-particle formation is observed but the basic characteristics such as a distinct nucleation mode or its growth are unclear, we classify the day as a class 3 event.

We calculated the annual NEE balances for 1997–2001 by first discarding unacceptable data points, then filling the resulting gaps ( $g$ ) in the time series with regressions based on the remaining accepted periods, and finally integrating all  $F_c$  values over each year. We selected data with two different methods: (1) by excluding the periods with low mixing according to the criteria described in Markkanen *et al.* (2001), usually  $u^* < 0.25$  m s<sup>-1</sup>; (hereon referred to as the “ $u^*$  method”); resulting amount of gaps  $g_M = 16\%$  for 1997–2001), and (2) by considering only the periods with simultaneous storage flux measurements, regardless of the level of mixing, as in one of the tests by Aubinet *et al.* 2002; (the “storage method”; resulting amount of gaps  $g_A = 3\%$ ). We excluded also polluted wind directions ( $g_{wd} = 5\%$ ), periods of instrument maintenance or malfunction ( $g_i = 6\%$ ) and, because of a false, negative offset in the measurements, all data for the three winters 1997–1998, 1998–1999, and

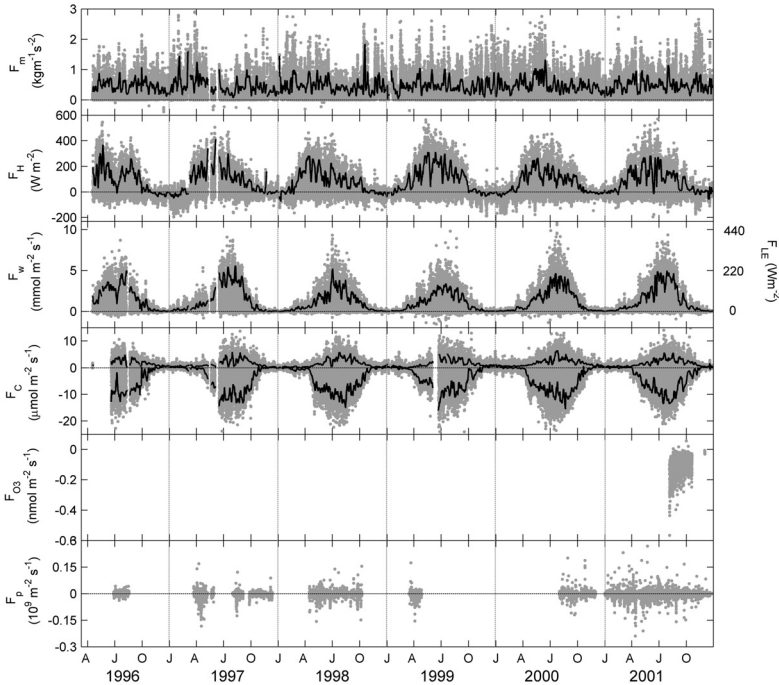


**Fig. 1.** Time series of surface fluxes in Hyttiälä, 1996–2001. Grey data points are half-hour averages. Black line is the average maximum flux (for 11:00–13:00, for  $F_C$  also for 01:00–03:00: the upper one) of the previous 5 days. The following fluxes were measured at 46.0 m in May 1999–June 2000 and at 23.3 m at other times:  $F_m$  = momentum flux,  $F_H$  = sensible heat flux,  $F_w$  = water vapour flux (also presented as  $F_{LE}$  = latent heat flux),  $F_C$  =  $CO_2$  flux including storage,  $F_{O_3}$  =  $O_3$  flux (measured at 22 m), and  $F_p$  = flux of aerosol particles in the size range of 14–600 nm (only at 23.3 m). Sign convention: < 0 downwards, > 0 upwards. However, for  $F_m$  > 0 downwards.

1999–2000 ( $g_w = 27\%$ ). The total amount of gaps for the period 1997–2001 in the  $u^*$  method was 54% ( $g_{wd} + g_i + g_w + g_M$ ) and in the storage method 41% ( $g_{wd} + g_i + g_w + g_A$ ). We calculated the regressions used for filling the gaps for each spring, summer, and autumn, and for nights and days separately. The single winter-time regression was based on the winters 1996–1997, 2000–2001 and 2001–2002.

## Results

According to the standard micrometeorological sign convention, we denoted downward flux from the atmosphere towards the forest negative and upward flux from the forest to the atmosphere positive. The only exception was  $F_m$  that is physically always directed downwards but is, conventionally, denoted positive. Contrary to the fluxes, the deposition velocities of  $O_3$

and particles ( $v_{d,O_3}$  and  $v_{d,p}$ , respectively) are traditionally denoted positive when deposition occurs downwards toward the surface. Because the different sign conventions may cause confusion, throughout this paper the terms ‘minimum’ and ‘maximum’ refer to values that are closest to zero and farthest from it, respectively, regardless of the sign.

## Annual patterns

Figures 1 and 2 show the entire time series of the measured surface fluxes and environmental variables in 1996–2001. In addition, for most quantities the highest daytime fluxes (11:00–13:00) averaged over the latest 5 days and denoted by a black line are superimposed on the time series. For  $CO_2$ , also the highest night-time fluxes (between 01:00–03:00, averaged over the latest 5 nights) are visible (Fig. 1).

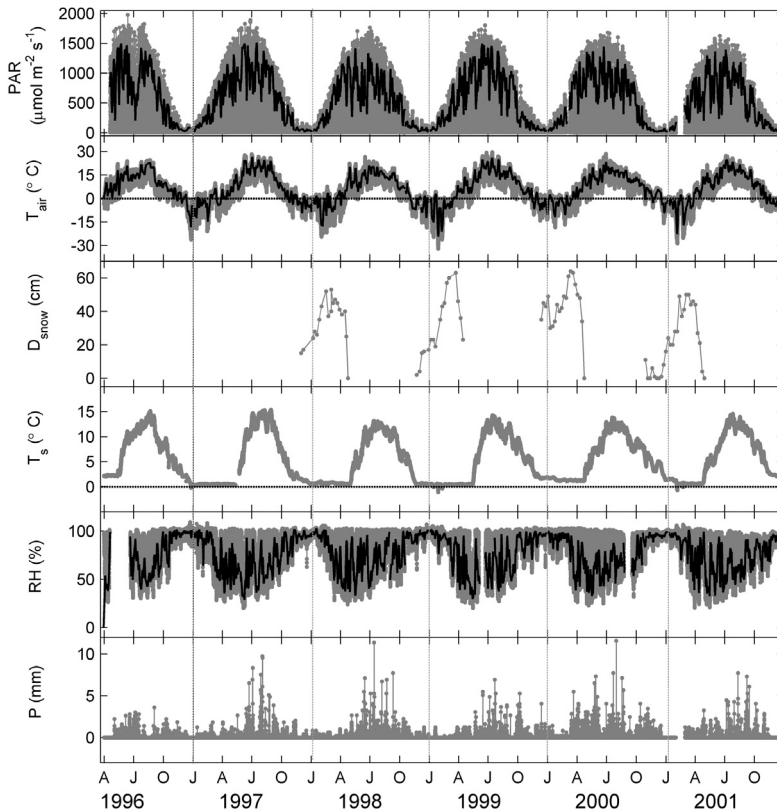


**Fig. 2.** Time series of environmental variables in Hyytiälä, 1996–2001. Grey data points are half-hour averages. Black line is the average maximum (11:00–13:00) of the previous 5 days. PAR = photosynthetically active radiation,  $T_{\text{air}}$  = air temperature at 8 m,  $D_{\text{snow}}$  = snow depth,  $T_{\text{s}}$  = soil temperature 5 cm below humus layer, RH = relative humidity at 16.8 m,  $P$  = cumulative precipitation per 30 min.

$F_{\text{H}}$ ,  $F_{\text{w}}$ , and  $F_{\text{C}}$  exhibited a clear annual pattern but  $F_{\text{m}}$  and  $F_{\text{p}}$  did not (Fig. 1). However,  $F_{\text{m}}$  was often slightly lower in July–September than at other times and generally ranged between 0 and  $1.5 \text{ kg m}^{-1} \text{ s}^{-2}$ . During the summers 1997 and 1998, it was particularly low, remaining below  $1 \text{ kg m}^{-1} \text{ s}^{-2}$  (corresponding approximately to  $u^* < 1 \text{ m s}^{-1}$ ) for 1.5 and 3 months, respectively.

$F_{\text{H}}$  ranged typically from  $-100$  to  $+50 \text{ W m}^{-2}$  in winter and from  $-100$  to  $+500 \text{ W m}^{-2}$  in summer (Fig. 1). Particularly low values ( $-180$  to  $-200 \text{ W m}^{-2}$ ) were observed during the winters 1996–1997

and 1999–2000.  $F_{\text{H}}$  increased very quickly in March (in 2001 already in February) and reached a maximum clearly before any other flux, already in April/May. A slow decrease started often already in July. The winter level was reached quite accurately when September turned to October, one to four weeks before the evapo-transpiration and the  $\text{CO}_2$  uptake effectively ended.

$F_{\text{w}}$  was mainly positive throughout the year, but close to zero during November–February (Fig. 1). With the first sign of snow melt  $F_{\text{w}}$  started to increase (Fig. 2), usually in February/March, four to eight weeks before significant  $\text{CO}_2$  uptake began and approximately at the same time as  $F_{\text{H}}$ . The spring increase of  $F_{\text{w}}$  was more step-like and more gradual than that of  $F_{\text{H}}$ . In July,  $F_{\text{w}}$  reached maximum values of 7 to  $10 \text{ mmol m}^{-2} \text{ s}^{-1}$  (corresponding to  $F_{\text{LE}}$  of 300 to  $440 \text{ W m}^{-2}$ ). In autumn, it decreased quickly at the end of October or at the beginning of November.

The wintertime  $F_{\text{C}}$  was small and mainly positive, ranging typically from  $-1$  to  $2 \text{ μmol m}^{-2} \text{ s}^{-1}$

**Table 1.** Cumulative NEE ( $\text{g(C) m}^{-2} \text{ yr}^{-1}$ ) calculated by two different methods, the  $u^*$  method and the storage method.

Year	$u^*$ method	Storage method
1997	-239	-307
1998	-233	-290
1999	-162	-232
2000	-168	-214
2001	-171	-230

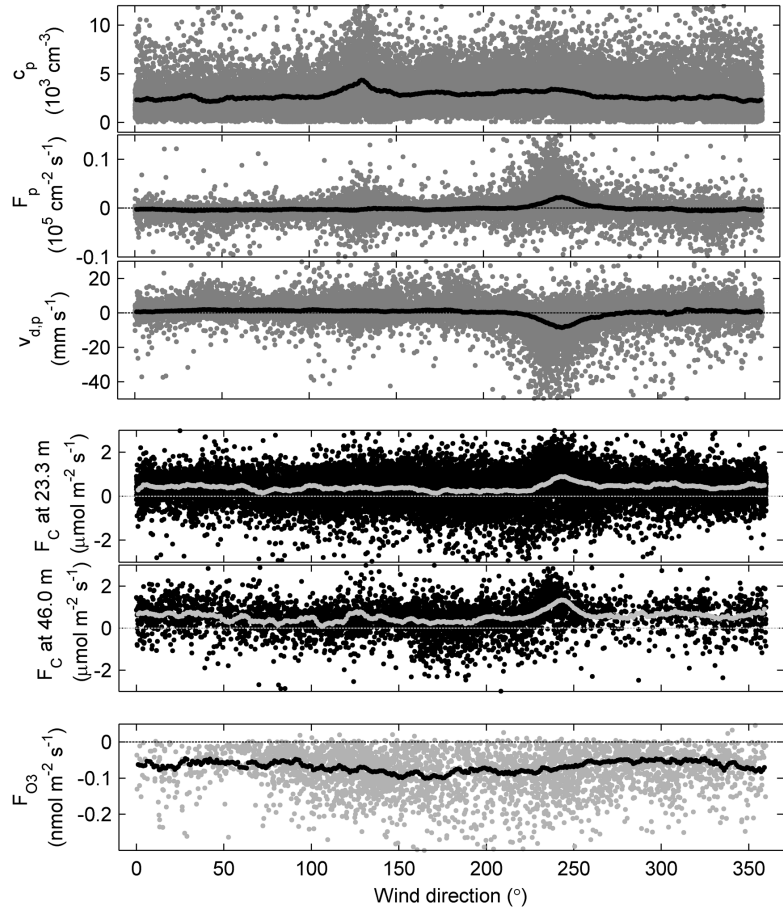


**Fig. 3.** Dependence on wind direction of aerosol particle concentration, flux and deposition velocity ( $c_p$ ,  $F_p$ , and  $v_{d,p}$ ), of  $\text{CO}_2$  flux ( $F_C$ ) at 23.3 m and 46.0 m in winters, and of  $\text{O}_3$  flux ( $F_{\text{O}_3}$ ) for August–October 2001. Points (dark grey for aerosol, black for  $\text{CO}_2$ , light grey for  $\text{O}_3$ ) are half-hour averages. The superimposed curve is the average calculated with wind direction intervals of  $1^\circ$ .

(Fig. 1). In spring, the daytime uptake (denoted negative) started to increase abruptly, and after a time lag of a few weeks also the night-time respiration (denoted positive) increased when the snow melt was complete and the soil temperature ( $T_s$ ) increased rapidly (Fig. 2). The uptake reached maximum values of  $-20$  to  $-25 \mu\text{mol m}^{-2} \text{s}^{-1}$  in late June/early July and the night-time respiration maximum values of  $10$  to  $15 \mu\text{mol m}^{-2} \text{s}^{-1}$ , again typically a few weeks later than did the uptake. The final diminishing of the daytime and night-time fluxes to the winter level happened rather simultaneously in late October–early November, at the same time as for  $F_w$ . The annual cumulative NEE obtained by the  $u^*$  method ranged from  $-239$  to  $-162 \text{ g(C) m}^{-2}$  and that obtained by the storage method from  $-307$  to  $-214 \text{ g(C) m}^{-2}$  (Table 1).

Even though no annual pattern could be deduced from a 3-month time series, it was

evident that  $F_{\text{O}_3}$ , directed entirely downwards towards the forest, decreased in strength during autumn (Fig. 1). The maximum downward  $F_{\text{O}_3}$  ranged from around  $-0.4 \text{ nmol m}^{-2} \text{s}^{-1}$  in the beginning of August to around  $-0.2 \text{ nmol m}^{-2} \text{s}^{-1}$  in mid October.

In the  $F_p$  time series the annual pattern was more difficult to discern, but both upward and downward fluxes were largest during spring (Fig. 1) when RH was at its lowest (Fig. 2).  $F_p$  ranged predominantly from  $-0.1$  to  $0.1 \times 10^9 \text{ particles m}^{-2} \text{s}^{-1}$ , that is, from  $-10^4$  to  $10^4 \text{ particles cm}^{-2} \text{s}^{-1}$ .

### Dependence on wind direction

The effect of wind direction was most evident in the particle data. The maximum particle concentration ( $c_p$ ) almost doubled when the wind came

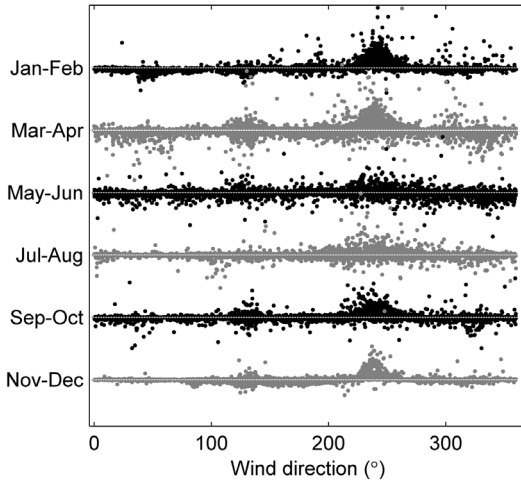


Fig. 4. Aerosol flux ( $F_p$ ) vs. wind direction for different months, 1997–2001.

from the direction  $120^\circ$ – $145^\circ$  (Fig. 3), where the nearest settlement, Korkeakoski (distance 8 km, population of 1000, a sawmill in the town centre), is situated. Negative and positive values of  $F_p$  also increased with that wind direction. For the direction of the SMEAR II station facilities,  $220^\circ$ – $260^\circ$ , positive values of  $F_p$  increased two- to three-fold. The aerosol deposition velocity ( $v_{d,p}$ ), defined as

$$v_{d,p} = -F_p/c_p, \quad (1)$$

was affected only by the direction of the station facilities which produced three to four times greater negative values of  $v_{d,p}$  than did the other directions. Figure 4 presents  $F_p$  for the years 1996–2001 as a function of wind direction for two months at a time. The effect of both the station facilities and of Korkeakoski almost vanished during the summer months May–August.

In  $F_C$ , a shift to the positive direction occurred in wintertime at the 23-m measurement level when the wind blew from the direction of the station facilities (Fig. 3). The effect was more pronounced at the height of 46 m: practically all fluxes were positive. We saw no effect at either height in summertime. Considering that the principal wind direction was from SW, we observed no clear wind direction dependence in the short time series of  $F_{O_3}$ , either (Fig. 3).

## Diurnal patterns

For comparison, Fig. 5 shows the median diurnal cycles of  $F_H$ ,  $F_w$ ,  $F_C$ ,  $F_{O_3}$ , and  $F_p$  as well as of  $c_p$ ,  $c_{O_3}$ ,  $v_{d,p}$ , and  $v_{d,O_3}$  for August 2001. At night,  $F_C$  was quite constant at  $3.5 \mu\text{mol m}^{-2} \text{s}^{-1}$ .  $F_C$  started decreasing at first daylight around 5:00 (Fig. 6). About an hour later, photosynthesis almost exceeded respiration and  $F_C$  was about to turn negative.  $F_C$  peaked at noon at  $-13 \mu\text{mol m}^{-2} \text{s}^{-1}$ . Subsequently, it decreased with decreasing PAR (photosynthetically active radiation,  $\lambda = 400$ – $800 \text{ nm}$ ) and returned to the night level again at 20:30, when the last beams of light disappeared.

$O_3$  did not exhibit a plateau of constant flux at night like  $CO_2$  did (Fig. 5). Instead,  $F_{O_3}$  and  $v_{d,O_3}$  towards the forest increased already right after the midnight minimums,  $-0.05 \text{ nmol m}^{-2} \text{s}^{-1}$  and  $2 \text{ mm s}^{-1}$ , respectively.  $v_{d,O_3}$  appeared to be at a maximum, around  $7.5 \text{ mm s}^{-1}$ , clearly before noon, between 8:00–11:00, and  $F_{O_3}$  a couple of hours later, between 10:00 and 13:00, with a downward maximum of around  $-0.22 \text{ nmol m}^{-2} \text{s}^{-1}$ .  $c_{O_3}$  had a minimum, 18 ppb, between 6:00 and 8:00 and a maximum, 31 ppb, around 13:00–16:00.

$F_p$  exhibited very little diurnal variation: between 12:00 and 19:00 when the relative humidity (RH) was at its lowest (50%–60%), the fluxes could be more negative than at other times, but the median was not clearly different (Figs. 5 and 6). In  $v_{d,p}$ , there was no diurnal variation but the general scatter was greater at daytime than at night.  $c_p$  had a weak diurnal pattern, decreasing from midnight until noon and then increasing again until midnight. Figure 7 shows some typical median diurnal cycles of aerosol particle properties for different seasons. During winter,  $c_p$  and  $F_p$  were small: In February 2001, the median  $c_p$  was about  $1.5$  to  $3 \times 10^3$  (particles)  $\text{cm}^{-3}$  and the median  $F_p$  fluctuated between  $0$  and  $-1.5 \times 10^3$  (particles)  $\text{cm}^{-2} \text{s}^{-1}$ . However, the average level of  $v_{d,p}$  was higher in winter than at any other time, around  $2.5 \text{ mm s}^{-1}$ , and the minimum and maximum  $v_{d,p}$  were  $1.5$  and  $6.5 \text{ mm s}^{-1}$ , respectively. In May 2001,  $c_p$  was about twice as large as in February, from  $3$  to  $4.5 \times 10^3$   $\text{cm}^{-3}$  except for a short but steep minimum of  $2 \times 10^3$   $\text{cm}^{-3}$  between 8:00 and 12:00. In May,  $F_p$  and

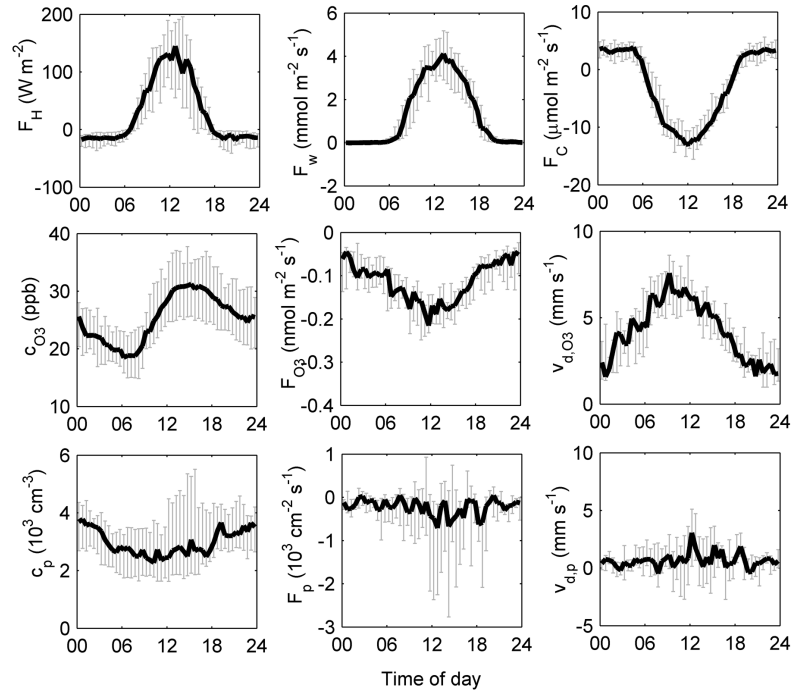


**Fig. 5.** Median diurnal cycle of fluxes, concentrations and deposition velocities in August 2001. Symbols as in Fig. 1. In addition: concentration of  $O_3$  and aerosol particles ( $c_{O_3}$ ,  $c_p$ ), deposition velocities for  $O_3$  and aerosol particles ( $v_{d,O_3}$ ,  $v_{d,p}$ ). Black line = monthly median of measurements for each half-hour moment, grey bars = monthly quartiles (top of the bars 75%, bottom 25%).

$v_{d,p}$  were at their largest between 12:00 and 18:00 and the diurnal pattern was very clear, although the upper and lower limits of the median  $F_p$  were the same as in February. However, the 25% and 75% quartiles in Fig. 7 show that variation of  $F_p$  around the median was considerable and that around noon, 25% of the flux was directed downwards with a rate larger than  $-3 \times 10^3 \text{ cm}^{-2} \text{ s}^{-1}$ . The variation around the median was not nearly as large in  $v_{d,p}$ , which ranged from 0 to 5  $\text{mm s}^{-1}$  in May. In July 1998, all three quantities were at their smallest, very close to zero. In September 1997, there was data only for a few days but the situation resembled that of May 2001, albeit on a slightly smaller scale.

### Aerosol formation events

Most new-particle formation events occurred in spring under RH from 30% to 70%, many also in summer and autumn (data not shown). Figure 8 presents the connection between new-particle formation events and  $v_{d,p}$ . The upper pane shows that the number frequency of  $v_{d,p}$  was symmetrically centred near zero on non-event days (black bars), with a mean and median  $v_{d,p}$  of 0.8 and 0.7

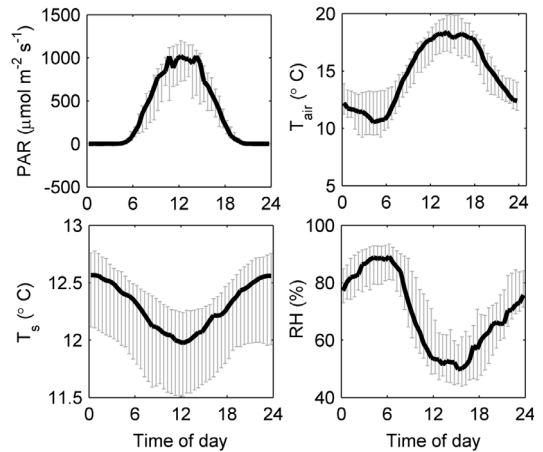


**Fig. 6.** Median diurnal cycles of PAR,  $T_{air}$ ,  $T_s$  and RH in August 2001. Symbols as in Fig. 2. Black line = monthly median of measurements for each half-hour moment, grey bars = monthly quartiles (top of the bars 75%, bottom 25%).

$\text{mm s}^{-1}$ , respectively. This is true also if we consider only the times when events on event days usually occur (6:15–19:45, grey bars). In this case, the mean and median  $v_{d,p}$  were both 0.7  $\text{mm s}^{-1}$ . The lower panel shows that on event days, however,  $v_{d,p}$  was much more often positive than

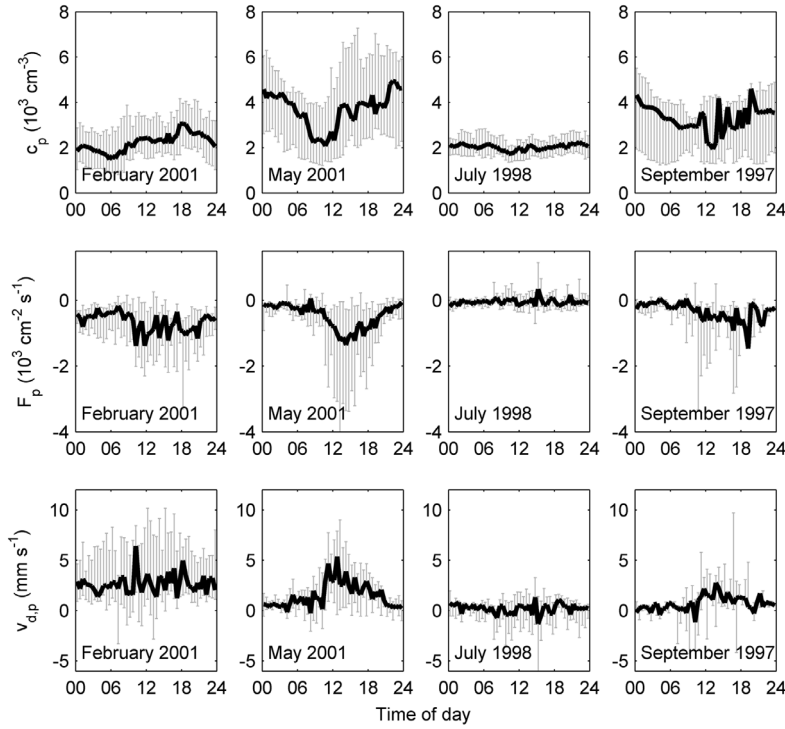


Fig. 7. Median diurnal cycles of aerosol particle concentrations, flux and deposition velocity in winter, spring, summer and autumn. Symbols as in Figs. 1 and 5.

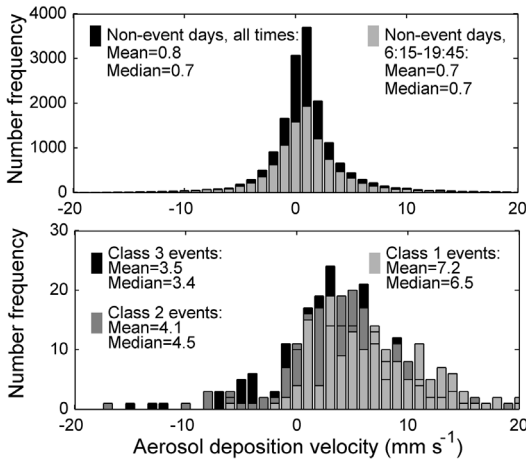


Fig. 8. Number frequency of aerosol particle deposition velocity ( $v_{d,p}$ ) on non-event and event periods in 1996–2001. Upper pane: non-event days, all hours (black bars); non-event-days, only hours 6:15–19:45 (grey bars). Lower pane: class 1, 2, and 3 new-particle formation events (light-grey, dark-grey and black bars, respectively) (see Material and methods for explanation).

negative. The mean and median  $v_{d,p}$  for the time periods with class 1 events were about 10 times higher than for non-event days, 7.2 and 6.5 mm

$s^{-1}$ , respectively. The number frequency of positive  $v_{d,p}$  was smaller for the less clear events, but even with class 3 events the mean and median were still 3.5 and 3.4 mm  $s^{-1}$ , four to five times as high as during non-event periods.

## Discussion

### Annual patterns

The variation in incoming energy and in the metabolic activity of vegetation and soil was evident in the annual patterns of  $F_C$ ,  $F_w$  and  $F_H$ . The fluxes were very small in winter and markedly larger in summer.  $F_m$  did not exhibit an annual pattern probably because the wind speed and roughness of the surface do not change very much over a year in a coniferous forest. The situation could be quite different in a deciduous forest where the leaves senesce for the winter and roughness characteristics change seasonally.

The quick increase of  $F_H$  in spring is the result of increased solar radiation that heats the surface and leads to the upward transport of

warm air. When the air is still cold, the warming of the surface leads to a large temperature gradient between the forest and the atmosphere and, consequently, to a large positive  $F_H$  in spring. Until plant metabolic activity and concurrent transpiration begin,  $F_w$  is small and mainly due to evaporation from the melting snow. Consequently, the outgoing energy is primarily transported by  $F_H$ . A measure of the partitioning of outgoing energy between  $F_H$  and  $F_w$  is the Bowen ratio ( $F_H/F_w$ ) that varies seasonally: In summer, increased transpiration leads to larger  $F_w$  and a smaller Bowen ratio (Markkanen *et al.* 2001).

The increase of the daytime uptake in the  $F_C$  time series in spring begins with increasing air temperatures and can vary by a month among years (Suni *et al.* 2003). A few weeks later, TER increases once the snow melts and the soil warms up, which was manifested in the time series as the increase of the night-time positive  $F_C$ . The forest was a net sink of carbon: The average annual cumulative NEE obtained by the  $u^*$  method was  $-195 \text{ g m}^{-2}$  and that obtained by the storage method  $-254 \text{ g m}^{-2}$ . The difference arises because the storage method assumes that advection (net horizontal transport) is negligible and does not affect the annual carbon mass balance. This is only true for terrain so flat that during low turbulence, the carbon that accumulates below the measurement level does not slide away along sloping ground undetected (night-time problem under low turbulence conditions, for details *see* Aubinet *et al.* 2000). In the  $u^*$  method, night-time low-turbulence values are discarded and replaced with modelled values based on measurements under similar but turbulent conditions. Since advection may not be neglected in Hyytiälä because of the slight sloping of the ground, the storage method is likely to overestimate the annual uptake, whereas the  $u^*$  method probably gives the least biased estimate.

For  $v_{d,O_3}$ , the main controlling factor during the growing season is the surface uptake resistance which, in daytime, is mainly stomatal. Towards winter,  $v_{d,O_3}$  decreases because the production and therefore the concentrations of  $O_3$  are reduced and the stomatal uptake of the vegetation diminishes. Moreover, the resistances of a coniferous forest canopy and ground

to  $O_3$  deposition are about 1.5 and 17.5 times higher with snow cover than without it, respectively (Seinfeld and Pandis 1998). Zeller (2000) reported even upward  $F_{O_3}$  from the surface of snow and postulated that  $O_3$  may be stored in the snow or in tree stands.

A large number of upward values were evident in  $F_p$  as expected from the work by Buzorius *et al.* 1998. They explained the upward flux by the existence of a particle source within or close to the canopy top. Also meteorological reasons such as concentration dilution during the early morning ABL growth (Nilsson *et al.* 2001) and roll circulation in the ABL (Buzorius *et al.* 2001) play a part. In many cases, the upward flux values result from a large random uncertainty of measurements.

Positive and negative maximum  $F_p$  were largest in spring (Fig. 1), but possible other annual patterns were effectively masked by changes in background concentration and size distribution. These changes are due to the different origins and trajectories of the air masses moving over the site, to the emissions from local and remote sources (*see* discussion on wind direction below), and to local aerosol formation.

## Dependence on wind direction

The emissions from local and remote anthropogenic sources had a significant effect on aerosol particle and  $CO_2$  concentrations and fluxes. Air coming from the nearest settlement, Korkeakoski (distance 8 km), brings with it a higher background concentration of particles. The SMEAR II station facilities are a local source in winter that increased the upward  $F_C$  at both measurement levels 1.5- to 2-fold and the upward  $F_p$  2- to 3-fold. In summer, the effects of the station facilities and of Korkeakoski on  $c_p$ ,  $F_p$  and  $F_C$  are weak because the need for heating the buildings is small and because the footprint area is smaller during the more turbulent summertime.

Especially in the case of trace gases and aerosols, the role of the more remote sources and of the air mass trajectories is important. Kulmala *et al.* (2000c) showed that the highest  $c_{O_3}$  come to Hyytiälä from the clean northern trajectory sectors in winter and from the polluted, south-

ern sectors in summer. Apparently, the polluted air masses from central Europe act as a sink in winter and as a source in spring and summer when the role of photochemistry becomes more important (Kulmala *et al.* 2000c). Accumulation-mode  $c_p$  is highest in the polluted, southern air masses, and local nucleation events occurred typically in clean air masses (Kulmala *et al.* 2000a, 2000c).

## Diurnal patterns

During daytime, the processes of respiration and photosynthesis act simultaneously. In Hyttiälä, optimal conditions for photosynthesis are approximately  $\text{PAR} > 800 \mu\text{mol m}^{-2} \text{s}^{-1}$  and  $15^\circ\text{C} \leq T_{\text{air}} \leq 20^\circ\text{C}$ . At higher temperatures, transpiration becomes too high, the stomata start to close and photosynthesis begins to decrease. Night-time TER increases with increasing  $T_{\text{air}}$  and  $T_s$  (Markkanen *et al.* 2001), but the factors affecting daytime TER are more difficult to analyse especially because we cannot infer TER from daytime NEE.

The diurnal range of  $v_{d,O_3}$  was similar (2–7  $\text{mm s}^{-1}$ ) in Hyttiälä as at a Scots pine forest site at Mekrijärvi in eastern Finland (0–7  $\text{mm s}^{-1}$ , Tuovinen *et al.* 2001) and at a Norway spruce forest site in Ulborg, Denmark in June 1994 (3.5–7  $\text{mm s}^{-1}$ , Pilegaard *et al.* 1995). In daytime,  $v_{d,O_3}$  is connected with PAR through stomatal uptake. That  $F_{O_3}$  and  $v_{d,O_3}$  towards the forest increased already right after midnight when no stomatal activity was present probably reflects the reactive nature of  $O_3$ . Possible reasons for this night-time decrease of  $c_{O_3}$  are surface deposition, potentially enhanced by terpenes on the surface and in the waxes of needles, and chemical reactions with  $\text{NO}_x$  or hydrocarbons such as monoterpenes. Even though the temperature-related emissions of monoterpenes from the vegetation decrease at night (Rinne *et al.* 2000, Kulmala *et al.* 2000a, Hakola *et al.* 2000), their concentrations increase because monoterpenes accumulate in the canopy during nights with low mixing and a shallow ABL (Rinne *et al.* 2000). The ensuing  $O_3$  sink near the surface is sustained if the characteristic times of  $O_3$  chemistry are fast compared with those of the low turbulent

transport. This is indeed the case according to the results of Keronen *et al.* (2003), which reveal the existence of a clear vertical profile in  $c_{O_3}$  with concentrations decreasing towards the surface. Moisture, such as the formation of dew on the surface of needles and other vegetation, could also provide an additional sink inside the canopy. This hypothesis agrees well with observations (Grantz *et al.* 1995, Finkelstein *et al.* 2000, Fuentes *et al.* 1992, 1994, Lamaud *et al.* 2002, Zhang *et al.* 2002).  $O_3$  itself is not particularly soluble and, in general, deposition on a water surface is limited by the solubility of the gas. However, if irreversible chemical reactions consume  $O_3$  molecules inside, say, a water film on a leaf, the concentration of  $O_3$  in the water does not increase and deposition can go on as long as the reactions take place (Sehmel 1980).

The diurnal pattern of  $c_p$  varied from non-existent in July 1998 (Fig. 7) to moderate in August 2001 (Fig. 5) and to strong in May 2001 (Fig. 7). At night,  $T_{\text{air}}$  decreases and the vapour pressures of organic hydrocarbons increase, resulting in enhanced condensation onto the surface of small nucleation-mode particles that thus grow into detectable sizes ( $> 14 \text{ nm}$ ). In the morning, the mixing starts and the particle concentrations are diluted in the deep daytime ABL.

A similar variation of the strength of the diurnal pattern was true also for  $F_p$  and  $v_{d,p}$ . During spring,  $F_p$  often remained close to zero at night and increased downwards by day as in May 2001 (Fig. 7). This kind of behaviour is typical for new-particle formation days (Buzorius *et al.* 2000). In autumn, the diurnal pattern could re-emerge for a few days but it was not nearly as clear or long lasting as in spring. Although we found no environmental variables that could explain or predict the diurnal pattern of  $F_p$  in general, in autumn its emergence seemed to be connected with the amount of radiation: In September 1997 and 2000 PAR was high and the diurnal pattern emerged, whereas in September 1998 and 2001 PAR was markedly smaller and no diurnal pattern appeared (data not shown).

The average  $v_{d,p}$  was highest in winter probably because the particles are smaller in winter when the amount of condensable vapour is small (Mäkelä *et al.* 2000).  $v_{d,p}$  is at its lowest for medium-sized particles with diameters between

0.1 and 1  $\mu\text{m}$  because in this size range the effect of both diffusion and gravitation is small (Seinfeld and Pandis 1998). Therefore, particles tend to accumulate in this size range (accumulation mode). Outside this range,  $v_{d,p}$  increases towards both smaller and larger sizes, respectively (Seinfeld and Pandis 1998, Raes *et al.* 2000).

## Aerosol formation events

New-particle formation is observed around 50 times a year at the Hyytiälä site (Kulmala *et al.* 2000a). Our results show that the average  $v_{d,p}$  towards the forest was greater on formation event days than on other days. This is because the nucleated particles are smaller than the more monodisperse, accumulation-mode particles that prevail during non-event conditions. This is in agreement with earlier findings based on short-term measurements in March–May 1997 (Buzorius *et al.* 2000). We found that the fraction of measurements indicating upward transport during non-event periods was 34%, during class 3 events 23%, during class 2 events 17%, and during class 1 events only 4%.

## Conclusions

The results show marked seasonal variations in  $F_H$ ,  $F_w$ , and  $F_C$  that stem from the seasonally varying amounts of incoming energy and metabolic activity. The effect of local and remote anthropogenic pollution is significant for  $c_p$ ,  $F_p$  and wintertime  $F_C$ .

The differing properties of the fluxes were evident: The inert nature of  $\text{CO}_2$  yields fluxes that follow environmental factors through plant physiology very closely and are relatively constant at night because, in order to be transported between the atmosphere and the biosphere,  $\text{CO}_2$  requires the active participation of plant and microbe metabolism. Fluxes of the reactive  $\text{O}_3$  depend on radiation in daytime, partly because of the local and regional photochemical production and destruction processes, but more importantly because  $\text{O}_3$  diffuses into the stomata and therefore depends on the plants' environment-controlled metabolic activity. At night,  $\text{O}_3$

concentrations, fluxes and deposition velocities change firstly because of surface deposition, enhanced by surface moisture and potentially by terpenes in the needle waxes, and secondly because of night sink reactions that are probably enhanced by the accumulation of monoterpenes near the surface. The aerosol flux, which exhibited no clear connection with any environmental variable, demonstrates the multireactive characteristics of aerosol particles that cannot be reduced into simple correlations. This resulted in practically no diurnal pattern at all, unless new-particle formation events occurred.

The formation of new nucleation-mode particles was manifested in  $v_{d,p}$ . The average downward  $v_{d,p}$  was greater on nucleation-event days because the small nucleation-mode particles have greater deposition velocities than do the larger accumulation-mode particles that prevail on non-event days.

Further studies should include the effect of surface wetness on trace gas and aerosol deposition.

*Acknowledgments:* The study was in part supported by the Academy of Finland and the EU projects Carboeuroflux, Carboage, CORE, and OSOA.

## References

- Atkinson R. 2000. Atmospheric chemistry of VOCs and  $\text{NO}_x$ . *Atmos. Environ.* 34: 2063–2101.
- Aubinet M., Heinesch B. & Longdoz B. 2002. Estimation of the carbon sequestration by a heterogeneous forest: night flux corrections, heterogeneity of the site and inter-annual variability. *Global Change Biology* 8: 1053–1071.
- Baldocchi D.D. & Vogel C.A. 1996. Energy and  $\text{CO}_2$  flux densities above and below a temperate broad-leaved forest and a boreal pine forest. *Tree Physiology* 16: 5–16.
- Burkhardt J., Kaiser H., Kappen L. & Goldbach H.E. 2001. The possible role of aerosols on stomatal conductivity for water vapour. *Basic and Applied Ecology* 2: 351–364.
- Buzorius G., Rannik Ü., Mäkelä J.M., Vesala T. & Kulmala M. 1998. Vertical aerosol particle fluxes measured by eddy covariance technique using condensational particle counter. *J. Aerosol Sci.* 29: 157–171.
- Buzorius G., Rannik Ü., Mäkelä J.M., Keronen P., Vesala T. & Kulmala M. 2000. Vertical aerosol fluxes measured by eddy covariance method and deposition of nucleation mode particles above a Scots pine forest in southern Finland. *J. Geophys. Res.* 105: 19905–19916.
- Buzorius G., Rannik Ü., Nilsson D. & Kulmala M. 2001.

- Vertical fluxes and micrometeorology during aerosol particle formation events. *Tellus* 53B: 394–405.
- Cajander A.K. 1909. Ueber Waldtypen. *Acta Forestalia Fennica* 1: 1–176.
- Calogirou A., Larsen B.R. & Kotzias D. 1999. Gas-phase terpene oxidation products: A review. *Atmos. Environ.* 33: 1423–1439.
- Finkelstein P.L., Ellestad T.G., Clarke J.F., Myers T.P., Schwede D.B., Hevert E.O. & Neal J.A. 2000. Ozone and sulphur dioxide dry deposition to forest: observations and model evaluation. *J. Geophys. Res.* 105: 15365–15377.
- Fuentes J.D., Gillespie T.J., Den Hartog G. & Neumann H.H. 1992. Ozone deposition onto a deciduous forest during dry and wet conditions. *Agricultural and Forest Meteorology* 62: 1–18.
- Fuentes J.D., Den Hartog G., Neumann H.H. & Gillespie T.J. 1994. Measurements and modelling of ozone deposition to wet foliage. In: Percy K.E., Cape J.N., Jagels R. & Simpson C.J. (eds.), *Air pollutants and the leaf cuticle*, NATO, ASI Series G: 36, pp. 239–253.
- Grantz D.A., Zhang X.J., Massman W.J., Den Hartog G., Neumann H.H. & Pederson J.R. 1995. Effects of stomatal conductance and surface wetness on ozone deposition in field-grown grape. *Atmos. Environ.* 29: 3189–3198.
- Grelle A., Lindroth A. & Mölder M. 1999. Seasonal variation of boreal forest surface conductance and evaporation. *Agricultural and Forest Meteorology* 98–99: 563–578.
- Hakola H., Laurila T., Rinne J. & Puhto K. 2000. The ambient concentrations of biogenic hydrocarbons at a northern European, boreal site. *Atmos. Environ.* 34: 4971–4982.
- Hämeri K., Laaksonen A., Väkevä M. & Suni T. 2001. Hygroscopic growth of ultrafine sodium chloride particles. *J. Geophys. Res.* 106: 20749–20758.
- Högberg P., Nordgren A., Buchmann N., Taylor A.F.S., Ekblad A., Högberg M.N., Nyberg G., Ottosson-Löfvenius M. & Read D.J. 2001. Large-scale forest girdling shows that current photosynthesis drives soil respiration. *Nature* 411: 789–792.
- Ilvesniemi H. & Liu C. 2001. Biomass distribution in a young Scots pine stand. *Boreal Env. Res.* 6: 3–8.
- Janson R., Rosman K., Karlsson A. & Hansson H.-C. 2001. Biogenic emissions and gaseous precursors to forest aerosols. *Tellus* 53B: 423–440.
- Jenkin M.E. & Clemitshaw K.C. 2000. Ozone and other secondary photochemical pollutants: chemical processes governing their formation in the planetary boundary layer. *Atmos. Environ.* 34: 2499–2527.
- Keronen P., Reissell A., Rannik Ü., Pohja T., Siivola E., Hiltunen V., Hari P., Kulmala M. & Vesala T. 2003. Ozone flux measurements at a Finnish forest site using the eddy covariance method. *Boreal Env. Res.* 8: 425–443.
- Kramer P.J. & Kozlowski T.T. 1979. Enzymes, energetics and respiration. In: *Physiology of woody plants*. Academic Press, New York. pp. 223–257.
- Kulmala M., Hämeri K., Mäkelä J.M., Aalto P.P., Pirjola L., Väkevä M., Nilsson E.D., Koponen I.K., Buzorius G., Keronen P., Rannik Ü., Laakso L., Vesala T., Bigg K., Seidl W., Forkel R., Hoffmann T., Spanke J., Janson R., Shimmo M., Hansson H.-C., O'Dowd C., Becker E., Paatero J., Teinilä K., Hillamo R., Viisanen Y., Laaksonen A., Swietlicki E., Salm J., Hari P., Altimir N. & Weber R. 2000a. Biogenic aerosol formation in the boreal forest. *Boreal Env. Res.* 5: 281–297.
- Kulmala M., Pirjola L. & Mäkelä J.M. 2000b. Stable sulphate clusters as a source of new atmospheric particles. *Nature* 404: 66–69.
- Kulmala M., Rannik Ü., Pirjola L., Dal Maso M., Karimäki J., Asmi A., Jäppinen A., Karhu V., Korhonen H., Malvikko S.-P., Puustinen A., Raittila J., Romakkaniemi S., Suni T., Yli-Koivisto S., Paatero J., Hari P. & Vesala T. 2000c. Characterization of atmospheric trace gas and aerosol concentrations at forest sites in southern and northern Finland using back trajectories. *Boreal Env. Res.* 5: 315–336.
- Kulmala M., Hämeri K., Aalto P.P., Mäkelä J.M., Pirjola L., Nilsson E.D., Buzorius G., Rannik Ü., Dal Maso M., Seidl W., Hoffman T., Janson R., Hansson H.-C., Viisanen Y., Laaksonen A. & O'Dowd C.D. 2001. Overview of the international project on biogenic aerosol formation in the boreal forest (BIOFOR). *Tellus* 53B: 324–343.
- Lamaud E., Carrara A., Brunet Y., Lopez A. & Druilhet A. 2002. Ozone fluxes above and within a pine forest canopy in dry and wet conditions. *Atmos. Environ.* 36: 77–88.
- Markkanen T., Rannik Ü., Keronen P., Suni T. & Vesala T. 2001. Eddy covariance fluxes over a boreal Scots pine forest. *Boreal Env. Res.* 6: 65–78.
- Mäkelä J.M., Hoffmann T., Holzke C., Väkevä M., Suni T., Mattila T., Aalto P.P., Tapper U., Kauppinen E.I. & O'Dowd C.D. 2002. Biogenic iodine emissions and identification of end-products in coastal ultrafine particles during nucleation bursts. *J. Geophys. Res.* 107 (D19), doi:10.1029/2001JD000580.
- Mäkelä J.M., Koponen I.K., Aalto P. & Kulmala M. 2000. One-year data of submicron size modes of tropospheric background aerosol in southern Finland. *J. Aerosol Sci.* 31: 595–611.
- Nilsson E. D., Rannik Ü., Kulmala M., Buzorius G. & O'Dowd C. 2001. Effects of the continental boundary layer evolution, convection, turbulence and entrainment on aerosol formation. *Tellus* 53B: 441–461.
- O'Dowd C., Aalto P., Hämeri K., Kulmala M. & Hoffmann T. 2002. Atmospheric particles from organic vapours. *Nature* 416: 497–498.
- Ottander C., Campbell D. & Öquist G. 1995. Seasonal changes in photosystem II organisation and pigment composition in *Pinus sylvestris*. *Planta* 197: 176–183.
- Peltola A. (ed.) 2001. *Metsätilastollinen vuosikirja*. Finnish Forest Research Institute, Vammala, 374 pp.
- Pilegaard K., Jensen N.-O. & Hummelshøj P. 1995. Seasonal and diurnal variation in the deposition velocity of ozone over a spruce forest in Denmark. *Water, Air, Soil Pollut.* 85: 2223–2228.
- Raes F., van Dingenen R., Vignati E., Wilson J., Putaud J.-P., Seinfeld J.H. & Adams P. 2000. Formation and cycling of aerosols in the global troposphere. *Atmos. Environ.* 34: 4215–4240.
- Rannik Ü. 1998. On the surface layer similarity at a complex

- forest site. *J. Geophys. Res.* 103: 8685–8697.
- Rinne J., Hakola H., Laurila T. & Rannik Ü. 2000. Canopy scale monoterpene emissions of *Pinus sylvestris* dominated forests. *Atmos. Environ.* 34: 2099–1107.
- Schmel G.A. 1980. Particle and gas dry deposition: a review. *Atmos. Environ.* 14: 983–1011.
- Seinfeld J. & Pandis S.N. 1998. *Atmospheric chemistry and physics: from air pollution to climate change*, John Wiley & Sons, New York, 1326 pp.
- Sevanto S., Vesala T., Perämäki M., Pumpanen J., Ilvesniemi H. & Nikinmaa E. 2001. Xylem diameter changes as an indicator of stand-level evapo-transpiration. *Boreal Env. Res.* 6: 45–52.
- Shaw R.H. & Finnigan J. 2002. The planetary boundary layer. In: *Advanced short course on agricultural, forest and micro meteorology*. Consiglio nazionale delle ricerche, Italy, pp. 3–12.
- Simpson D., Ashmore M., Emberson L., Tuovinen J.-P., MacDougall M. & Smith R.I. 2002. Stomatal ozone uptake over Europe: preliminary results. In: *Trans-boundary acidification, eutrophication and ground level ozone in Europe*. EMEP Report 1&2/2002, Norwegian Meteorological Institute, Oslo, pp. 63–71.
- Suni T., Berninger F., Markkanen T., Keronen P., Rannik Ü. & Vesala T. 2003. Interannual variability and timing of growing-season CO<sub>2</sub> exchange in a boreal forest. *J. Geophys. Res.* 108 (D9), doi:10.1029/2002JD002381.
- Tuovinen J.-P., Simpson D., Mikkelsen T.N., Emberson L.D., Ashmore M.R., Aurela M., Cambridge H.M., Hovmand M.F., Jensen N.O., Laurila T., Pilegaard K. & Ro-Poulsen H. 2001. Comparisons of measured and modelled ozone deposition to forests in northern Europe. *Water, Air, Soil Pollut., Focus* 1: 263–274.
- Vesala T., Haataja J., Aalto P., Altimir N., Buzorius G., Garam E., Hämeri K., Ilvesniemi H., Jokinen V., Keronen P., Lahti T., Markkanen T., Mäkelä J.M., Nikinmaa E., Palmroth S., Palva L., Pohja T., Pumpanen J., Rannik Ü, Siivola E., Ylitalo H., Hari P. & Kulmala M. 1998. Long-term field measurements of atmosphere-surface interactions in boreal forest combining forest ecology, micrometeorology, aerosol physics and atmospheric chemistry. *Trends in Heat, Mass and Momentum Transfer* 4: 17–35.
- Volz A. & Kley D. 1988. Ozone measurements in the 19th century: an evaluation of the Montsouris series. *Nature* 332: 240–242.
- Yu H., Liu S.C. & Dickinson R.E. 2002. Radiative effects of aerosols on the evolution of the atmospheric boundary layer. *J. Geophys. Res.* 107 (D12), doi:10.1029/2001JD000754.
- Zeller K. 2000. Wintertime ozone fluxes and profiles above a subalpine spruce–fir forest. *J. Appl. Meteor.* 39: 92–101.
- Zhang L., Brook J.R. & Vet R. 2002. On ozone dry deposition — with emphasis on non-stomatal uptake and wet canopies. *Atmos. Environ.* 36: 4787–4799.

Received 4 February 2003, accepted 22 July 2003